Polymer Chemistry

RSC Publishing

PAPER

View Article Online
View Journal | View Issue

Cite this: *Polym. Chem.*, 2013, **4**, 2025

Functional copolymer brushes composed of a hydrophobic backbone and densely grafted conjugated side chains *via* a combination of living polymerization with click chemistry†

Xinchang Pang, Lei Zhao, Chaowei Feng, Ruifeng Wu, Haihong Ma and Zhiqun Lin*

Received 18th December 2012
Accepted 3rd January 2013

DOI: 10.1039/c2py21124f

www.rsc.org/polymers

A series of well-defined copolymer brushes, PS-*g*-P3HT, composed of a hydrophobic coil-like PS backbone and densely grafted rod-like P3HT side chains were successfully synthesized by a combination of the quasi-living Grignard metathesis (GRIM) method, reversible addition–fragmentation chain transfer (RAFT), and click reaction. The molecular weight distribution of the resulting PS-*g*-P3HT copolymer brushes was rather narrow (polydispersity index, PDI < 1.2). The grafting efficiency was very high (*i.e.*, the efficiency of all click reactions >96%). The self-assembly of PS-*g*-P3HT at the air/water interface was explored using the Langmuir–Blodgett (LB) technique. Quite intriguingly, circular domain arrays composed of the non-crystallized P3HT nanofibers were observed at high surface pressure.

Introduction

Copolymer brushes composed of a flexible linear backbone and densely grafted side chains are a unique class of graft copolymers.[1] Steric repulsion between polymeric side chains forces the backbone of copolymer brushes to adopt an extended chain conformation. When the length of the backbone is longer than that of the side chain, copolymer brushes possess a cylindrical shape in solution.[2] Due to the distinctive chemical and physical properties originating from their intrinsically complex architecture, copolymer brushes have received much attention to better understand the architecture–property relationship[1,3] for potential applications in supramolecular science, biomaterials, advanced materials (*e.g.*, supersoft elastomers),[4] photonic crystals,[5] *etc.* The utilization of these copolymer brushes allows for the development of molecular tensile machines when interacting with the surface,[6] the creation of organic nanowires[7] and nanotubes,[8] and the formation of inorganic nanoparticles and nanowires by capitalizing on copolymer brushes as templates.[7]

Generally, there are three methods to yield copolymer brushes, namely, grafting-through, grafting-onto, and grafting-from.[9] For the grafting-through method, macromonomers are first synthesized and then homopolymerized or copolymerized with other monomers. In the grafting-onto approach, the backbone with reactive sites and side chains with functional end groups are first prepared separately, and then the copolymers are formed *via* a coupling reaction between them. By contrast, in the grafting-from approach, the side chains are grown from the polymer backbone with pendant multi-initiation sites; the easy purification of the resulting polymer brushes is the peculiarity of this method, and pure polymer brushes are of key importance to explore their self-assembly at the air/water interface.

Recent advances in various polymerization techniques, such as ring opening metathesis polymerization (ROMP),[10–12] controlled radical polymerization,[13–15] including atom transfer radical polymerization (ATRP),[16,17] nitroxide-mediated polymerization (NMP),[18–20] and reversible addition–fragmentation chain transfer (RAFT) polymerization,[21–24] enable the synthesis of functional copolymers with well-defined yet complex architectures. Notably, most of reported copolymer brushes have been prepared by ROMP,[10,11] ATRP and NMP;[18,25] by contrast, RAFT is widely recognized as a versatile method to yield polymers from a myriad of monomers under a broad range of experimental conditions, especially for monomers with active functional groups (*e.g.*, carboxyl group, Br, Cl, *etc.*).[26,27]

Conjugated polymers such as poly(3-alkylthiophenes) (P3AT) have been considered as promising materials for use in solar cells, organic field effect transistors, electrochromic devices, smart windows, and biosensors.[28–33] Among the various types of conjugated polymers, regioregular poly(3-hexylthiopene) (P3HT) is one of the most heavily studied organic semiconductors due to its superior optoelectronic properties, good solubility in most non-polar solvents, chemical and thermal stabilities, and very low toxicity.[34–36] P3HT consists of a rather rigid backbone with a regular head-to-tail arrangement of

School of Materials Science and Engineering, Georgia Institute of Technology, Atlanta, GA 30332, USA. E-mail: zhiqun.lin@mse.gatech.edu; Fax: +1 404-385-3734; Tel: +1 404-385-4404

† Electronic supplementary information (ESI) available. See DOI: 10.1039/c2py21124f

pendant hexyl side chains that allow for efficient π–π stacking of the conjugated backbones and solubilization.[37–43] To date, a variety of P3HT-containing *linear* rod–coil block copolymers have been synthesized by combining Grignard metathesis (GRIM) reaction with controlled radical polymerization, leading to the formation of a unique nanostructured assembly and the resulting electronic activity.[44,45] However, *limited* work has been performed on the preparation of copolymer brushes composed of P3HT as side chains as it is quite challenging to synthesize linear macroinitiators with multi-initiation sites on the polymer backbone and grow conjugated polymer P3HT at the initiation sites.[46,47]

Herein, we report a *facile* route to a series of intriguing copolymer brushes composed of a hydrophobic coil-like polystyrene (PS) backbone and densely grafted rod-like P3HT side chains (denoted PS-*g*-P3HT) with well-defined molecular architectures, molecular weights, and the ratio of two dissimilar blocks *via* a judicious combination of RAFT polymerization, quasi-living GRIM, and click reaction. Due to the versatility and simple experimental conditions of RAFT polymerization, in conjunction with the high specificity, quantitative yield and nearly perfect fidelity of click reaction,[48–50] this simple yet robust synthetic approach opens up new avenues for preparing a wide diversity of P3HT-based copolymer brushes with different polymer backbones as well as other copolymer brushes consisting of different polymer backbones and conjugated side chains other than P3HT. Thus, it offers great promise for exploring the fundamental relationship between the brush-like architectures and their properties in solution and solid states. Subsequently, the self-assembly of these novel PS-*g*-P3HT copolymer brushes at the air/water interface formed by the Langmuir–Blodgett (LB) technique was explored. To the best of our knowledge, this is the *first study* of self-assembly of P3HT-based copolymer brushes at the air/water interface yielding intriguing conjugated polymer surface morphology. The possible models were proposed to understand the self-assembly and photoluminescence behaviors of the thin PS-*g*-P3HT copolymer brush film. Such conjugated polymer-containing copolymer brushes promise new opportunities for designing organic rod-like and tubular structures of nanometer dimensions and potential applications in biomaterials, supramolecular science, polymer-hybrid nanocomposites, nanotechnology, and so on.[8]

Experimental section

Materials

N,*N*,*N*′,*N*″,*N*‴-Pentamethyldiethylene triamine (PMDETA, 99%), sodium azide (≥99.5%), 2,5-dibromo-3-hexyl-thiophene (97%), *tert*-butyl magnesium chloride (2.0 M solution in diethyl ether), [1,3-bis(diphenyl phosphino)propane]dichloronickel(II) ($Ni(dppp)Cl_2$) and ethynyl magnesium bromide (0.5 M solution in tetrahydrofuran) were purchased from Sigma-Aldrich and used as received. CuBr (98%, Sigma-Aldrich) was stirred overnight in acetic acid and filtered, washed with ethanol and diethyl ether successively, and dried *in vacuo*. 4-(Chloromethyl)styrene (Sigma-Aldrich, 90%) and *N*,*N*-dimethyl formamide (DMF, Fisher Scientific, 99.9%) were dried over calcium hydride for 48 h and distilled under reduced pressure just before use. Tetrahydrofuran (THF, 99%) was refluxed over a potassium wire and distilled from potassium naphthalenide solution. 2,2-Azobisisobutyronitrile (AIBN) was recrystallized from methanol twice. The RAFT agent, 2-phenylprop-2-yl dithiobenzoate (PPDTB), was prepared as described in ref. 51 in the yield of 48.6%, ^{1}H-NMR ($CDCl_3$, d(ppm)): 2.01 (s, 6H); 7.16–7.55 (m, 8H) and 7.85 (m, 2H). All other reagents were purified by common purification procedures.

Preparation of poly(4-(chloromethyl)styrene) by RAFT polymerization

A linear polymer, poly(4-(chloromethyl)styrene) (P(S-Cl)) was prepared by the RAFT polymerization[52,53] of 4-(chloromethyl) styrene in toluene, using AIBN as an initiator and PPDTB as a chain transfer agent. In a typical process, an ampoule charged with AIBN (0.04 mmol; 6.6 mg), PPDTB (0.12 mmol; 32.7 mg), 4-(chloromethyl)styrene monomer (0.1 mol; 15.262 g), and toluene (16 mL) was vacuumed by three freeze–thaw cycles at the temperature of liquid nitrogen, then sealed and placed in a constant temperature oil bath at 70 °C for a given time (see Table 1), then the polymerization was stopped by immersing the reaction ampoule into an ice bath for half an hour. Then, the product mixture was precipitated in cold dried methanol. The product was purified by dissolution/precipitation with THF/methanol and then dried to a constant weight under vacuum at 60 °C.

Preparation of poly(4-(azidemethyl)styrene) (P(S-N_3))

The chlorine atoms in each repeating unit of P(S-Cl) were converted into azides by reacting with sodium azide in DMF. The linear polymer, P(S-Cl) (3.0 g) was dissolved in DMF (15 mL), and sodium azide (Cl in polymer : sodium azide = 1 : 10; molar ratio) was added to the solution. The reaction mixture was stirred for 24 h at room temperature. Dichloromethane (25.0 mL) was added into the mixture, and the mixture was washed three times with distilled water. The organic layer was dried with anhydrous $MgSO_4$, and the solvent was removed by vacuum. The product was then collected and dried at 40 °C in a vacuum oven for 4 h (yield = 80.6%).

Table 1 Summary of poly(4-(chloromethyl)styrene)

Entry	Time (h)	Conv.[a] (%)	$M_{n,GPC}$[b] (g mol^{-1})	M_w/M_n[c]	$M_{n,NMR}$[d] (g mol^{-1})
Sample-1	5	3.38	5200	1.09	4300
Sample-2	10	9.64	14 400	1.07	12 260
Sample-3	15	15.24	21 900	1.11	19 380
Sample-4	20	19.33	26 950	1.08	24 580
Sample-5	30	26.05	35 600	1.12	33 130

[a] Determined by the gravimetric method. [b] Number-average molecular weight determined by GPC, calibrated against PS standard. [c] The polydispersity index determined by GPC. [d] Number average molecular weight (M_n) calculated from the ^{1}H-NMR data: $M_{n,NMR} = \frac{A_m/2}{A_a/6} \times 152.62$, where A_m and A_a represent the integral area of the methylene protons in the repeating unit of poly(4-(chloromethyl)-styrene) and the integral area of methyl protons at the α-end of poly(4-(chloromethyl)styrene) (Fig. 3(I)), respectively, and 152.62 is the molecular weight of the 4-(chloromethyl)styrene monomer.

Synthesis of ethynyl-terminated P3HT

Ethynyl-terminated P3HT was synthesized by a quasi-living Grignard metathesis (GRIM) method.[29,30,54,55] Briefly, 2,5-dibromo-3-hexylthiophene (0.815 g, 2.5 mmol) was dissolved in THF (5 mL) in a three-neck flask and stirred under Ar. *tert*-Butylmagnesium chloride (1.25 mL, 2.5 mmol) was added *via* a syringe. The mixture was stirred for 2 h at room temperature. Subsequently, it was diluted to 25 mL with THF and Ni(dppp)Cl_2 (22.5 mg, 0.041 mmol) was added. The resulting mixture was first stirred for 10 min at room temperature, producing intermediate P3HT, followed by reacting with ethynylmagnesium bromide (2 mL, 1 mmol) in THF for 30 min. The ethynyl-terminated P3HT was obtained by precipitating the reaction mixture in methanol, filtering in an extraction thimble, and washing by Soxhlet extraction with methanol, hexanes, and chloroform sequentially. The final pure ethynyl-terminated P3HT was recovered after chloroform was evaporated. The regioregularity of P3HT was greater than 98% as determined by ^{1}H-NMR. The number average molecular weight and PDI of ethynyl-terminated P3HT were 5100 g mol^{-1} (based on ^{1}H-NMR), 4100 g mol^{-1} (based on GPC) and 1.18 (GPC), respectively.

Yield: 40.8%. ^{1}H-NMR ($CDCl_3$, d (ppm)): 6.98 (s, 1H), 3.05 (s, 1H), 2.8 (t, $J = 3$ Hz, 2H), 1.7 (m, 2H), 1.43 (m, 2H), 1.36 (m, 4H), and 0.92 (t, 3H).

Synthesis of copolymer brush PS-*g*-P3HT by click reaction

P(S-N_3) and ethynyl-terminated P3HT were dissolved in DMF (10 mL) in a dry ampoule. CuBr and PMDETA were added, and the reaction mixture (ethynyl-terminated P3HT : –N_3 in P(S-N_3) : copper bromide : PMDETA = 1.2 : 1 : 10 : 10; molar ratio) was degassed by three freeze–pump–thaw cycles and left under nitrogen. The ampoule was immersed in an oil bath at 90 °C for 24 h, then taken from the oil bath and dipped in liquid nitrogen to stop the reaction. The products were diluted with THF, and the solution was passed through an alumina column to remove the copper salt, precipitated in cold methanol, and dried in a vacuum oven at 40 °C for 4 h. The copolymer brush PS-*g*-P3HT was thus obtained.

Preparation of a Langmuir film at the air/water interface

PS-*g*-P3HT (sample-b in Table 2) chloroform solutions at the concentration $c = 1$ mg mL^{-1} were prepared. The surface pressure–area (π–A) isotherms and thin copolymer brush film were obtained with an R&K Langmuir–Blodgett (LB) system (Riegler & Kirstein, GmbH, 160 cm^2 Teflon trough). Prior to the LB study, the LB trough was carefully cleaned with 1 : 1 H_2O_2 : NH_3OH solution overnight and subsequently rinsed with DI water (NanoPure, >18 MΩ cm) 5 times. A 15 μL chloroform solution was gently placed on the water surface to ensure the initial gas state. After the solvent evaporated for 30 min, the monolayer film was compressed at a rate of 150 μm s^{-1}. The Si substrate used for depositing LB films was cleaned with a mixture of sulfuric acid and Nonchromix, followed by rinsing with DI water and blown dry with N_2. For LB depositions, the Si substrate was withdrawn at a rate of 35 μm s^{-1} while keeping the pressure constant.

Table 2 Summary of PS-*g*-P3HT copolymer brushes

Entry[a]	$M_{n,GPC}$[b] (g mol^{-1})	M_w/M_n[c]	$M_{n,NMR}$[d] (g mol^{-1})	Yield (%)	Efficiency[e] (%)
Sample-a	31 900	1.15	143 720	76.9	96.9
Sample-b	64 600	1.17	416 330	82.6	98.5
Sample-c	94 300	1.18	653 580	85.2	97.8
Sample-d	113 900	1.16	831 400	83.4	98.1
Sample-e	146 200	1.19	1 113 960	81.8	97.5

[a] Five samples (a–e) were prepared by click reaction between ethynyl-terminated P3HT and sample-1, sample-2, sample-3, sample-4, and sample-5 (see Table 1), respectively. [b] Number-average molecular weight determined by GPC, calibrated against PS standard. [c] The polydispersity index determined by GPC. [d] Number average molecular weight (M_n) calculated from the ^{1}H-NMR data: $M_{n,NMR} = \frac{M_{n,NMR,P(S\text{-}Cl)}}{152.62} \times \left(\frac{A_m/3}{A_e/2} \times 166.3 + 159.2 \right)$, where A_m and A_e represent the integral area of the methyl protons in the repeating unit of P3HT (side chains in PS-*g*-P3HT) and the integral area of methylene protons in the repeating unit of poly(4-(chloromethyl)styrene) (backbone in PS-*g*-P3HT) (Fig. 3(III) and S1†), respectively; 152.62, 159.2 and 166.3 are the molecular weights of 4-(chloromethyl)styrene monomer, 4-(azidemethyl)styrene, and the repeating unit of P3HT, respectively; and $M_{n,NMR,P(S\text{-}Cl)}$ is number-average molecular weight of P(S-Cl) based on ^{1}H-NMR (Table 1). [e] Efficiency of click reaction (E_T), calculated from ^{1}H-NMR spectra of the PS-*g*-P3HT copolymer brushes and P(S-Cl).

Characterizations

The molecular weights of polymers were measured using an Agilent1100 GPC equipped with a G1310A pump, a G1362A refractive detector, and a G1314A variable wavelength detector. THF was used as the eluent at 35 °C at 1.0 mL min^{-1}. One 5 μm LP gel column and two 5 μm LP gel mixed bed columns were calibrated with polystyrene standard samples. ^{1}H-NMR spectra were obtained with a Varian VXR-300 spectrometer. $CDCl_3$ was used as the solvent. FT-IR spectra were collected on a Magna-550 Fourier transform infrared spectrometer. The morphologies of LB films were examined by Atomic Force Microscopy (AFM; Dimension 3000) in the tapping mode. The scanning rate was 2 Hz. Each sample was imaged at more than 5 locations to ensure the reproducibility of the features observed. The detailed morphology of the samples was determined by TEM measurements (JEOL 1200EX scanning/transmission electron microscope (STEM); operated at 80 kV). The photoluminescence spectra were taken with a Nikon Eclipse TE2000-E microscope coupled with an optical insights hyperspectral unit and a Cascade 512B camera (Roger Scientific), chloroform was used as a solvent when the solution sample was characterized.

Results and discussions

Preparation of poly(4-(azidemethyl)styrene) (P(S-N_3))

As depicted in Scheme 1a, poly(4-(chloromethyl)styrene) (P(S-Cl)) was first synthesized. The polymerization of

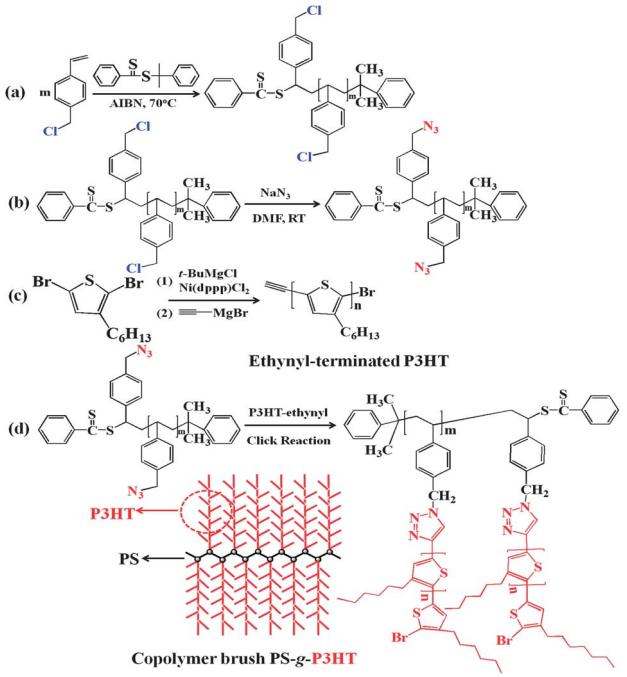

Scheme 1 Schematic representation of the synthetic route to novel copolymer brush PS-*g*-P3HT. Synthesis of (a) poly(4-(chloromethyl)styrene) (P(S-Cl)), (b) poly(4-(azidemethyl)styrene) (P(S-N_3)), and (c) ethynyl-terminated P3HT, respectively. (d) Formation of the PS-*g*-P3HT copolymer brush by click reaction between P(S-N_3) and ethynyl-terminated P3HT.

4-(chloromethyl)styrene monomer was carried out by a RAFT process in which 2-phenylprop-2-yl dithiobenzoate (PPDTB) was used as a chain transfer agent. Five polymers with different molecular weights (MWs) were yielded by varying the polymerization time (Table 1). The relationship of the monomer conversion with the MW and MW distribution is shown in Fig. 1, in which the MW increased with the monomer conversion and the MW distribution was less than 1.2. Clearly, the polymerization of 4-(chloromethyl)styrene in the presence of PPDTB was highly controllable.

Fig. 2 illustrates the GPC traces of P(S-Cl) samples obtained with different polymerization times. It is clear that the peaks shifted to higher MWs as the reaction time increased. The

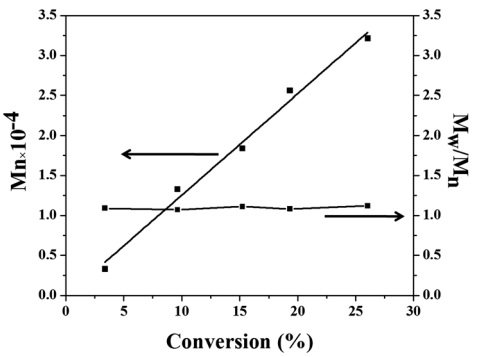

Fig. 1 The dependence of M_n and M_w/M_n on the conversion of 4-(chloromethyl) styrene in the RAFT polymerization.

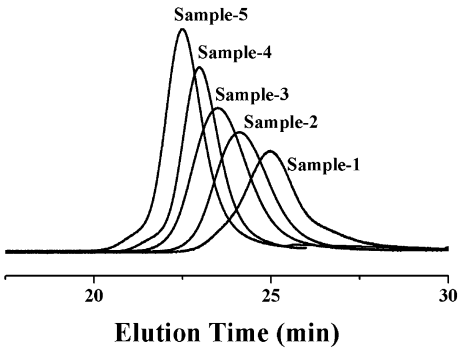

Fig. 2 GPC traces of poly(4-(chloromethyl)styrene) (see Table 1).

MWs of polymers derived from ^{1}H-NMR were different from those obtained from GPC due to different hydrodynamic volumes of samples in comparison to the linear polystyrene standard in GPC columns. Fig. 3(I) displays a typical ^{1}H-NMR spectrum of P(S-Cl). The chemical shifts at δ = 6.33–7.31 ppm are assigned to the protons of phenyl rings of the polystyrene backbone, at δ = 4.51 ppm (peak m, 2H) can be assigned to the methylene protons of the repeating unit of P(S-Cl) (*i.e.*, –C**H**$_2$–Cl).

Subsequently, poly(4-(azidemethyl)styrene) (P(S-N_3)) with different MWs was synthesized by the reaction of P(S-Cl) with sodium azide in DMF at room temperature (Scheme 1b). The ^{1}H-NMR spectrum of the resulting P(S-N_3) is shown in Fig. 3(II). A strong characteristic peak at δ = 4.23 ppm (*i.e.*, peak n′) represented the methylene protons in the repeating unit of P(S-N_3) (*i.e.*, –C**H**$_2$–N_3). The transformation of chlorine atoms to the azide group was also corroborated by the emergence of a signal at δ = 4.51 ppm (*i.e.*, peak m′, –C**H**$_2$–Cl, repeating unit of P(S-Cl)) shifting to δ = 4.23 ppm (*i.e.*, peak n′). Furthermore, P(S-N_3) displayed the characteristic stretching band of –N_3 which appeared at 2112 cm^{-1} in the IR spectrum (Fig. S2†).

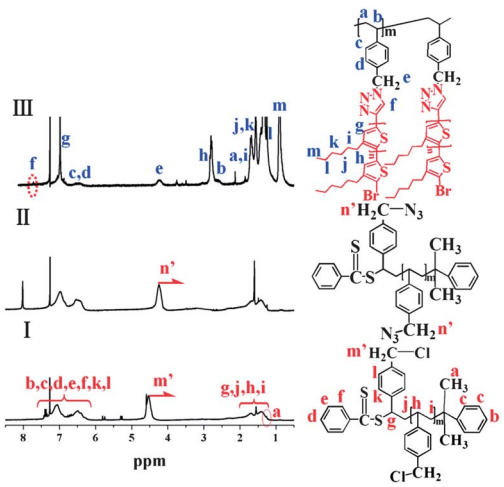

Fig. 3 ^{1}H-NMR spectra: (I) poly(4-(chloromethyl)styrene), (II) poly(4-(azidemethyl)styrene) (*i.e.*, sample-2 in Table 1), and (III) PS-*g*-P3HT copolymer brush (*i.e.*, sample-b in Table 2) in $CDCl_3$.

Synthesis of copolymer brush PS-*g*-P3HT by click reaction

The ethynyl-terminated P3HT was synthesized by end-capping P3HT prepared by the GRIM method with ethynylmagnesium bromide (Scheme 1c). Finally, 1,3-dipolar cycloaddition (copper-catalyzed azide–alkyne cycloaddition) between ethynyl-terminated P3HT and P(S-N_3) (*i.e.*, click reaction) yielded PS-*g*-P3HT copolymer brushes (Scheme 1d). The click reaction was performed in the presence of CuBr/*N*,*N*,*N*′,*N*″,*N*″-pentamethyldiethylene triamine (PMDETA) in DMF at 90 °C. The obtained copolymer brushes are summarized in Table 2. Click reactions possess several attractive features, including an extremely versatile bond-formation process, no need for protecting groups, good selectivity, nearly complete conversion, and generally no need for purification. As such, it stands out as a promising method to simplify the synthetic procedure and provides opportunities to increase the grafting density for large-scale synthesis.[48–50,56]

The success of the formation of PS-*g*-P3HT copolymer brushes was verified by ^{1}H-NMR, IR spectroscopy, and GPC. In comparison to the ^{1}H-NMR spectrum of P(S-N_3) (Fig. 3(II)), a new signal (*i.e.*, f) associated with the triazole ring at $\delta = 7.76$ ppm appeared in the PS-*g*-P3HT copolymer brush (Fig. 3(III)), suggesting that the click reaction between the azide group of P(S-N_3) and the alkyne group of ethynyl-terminated P3HT was accomplished. The transformation of the azide group to a triazole ring was also confirmed by the emergence of a signal at $\delta = 4.23$ ppm (*i.e.*, n′ in Fig. 3(II), –C***H***$_2$–N_3, repeating unit of P(S-N_3)) shifting to $\delta = 4.19$ ppm (*i.e.*, e in Fig. 3(III)). In addition, the proton (b) in PS-*g*-P3HT shifted to a low field compared to the same proton (h) in P(S-Cl) (Fig. 3(I)) after click reaction, which was in accordance with the recent report.[52] Fig. 3(III) also shows the characteristic peaks of the thiophene group of P3HT at $\delta = 6.98$ ppm (*i.e.*, g in Fig. 3(III)), hexyl group of P3HT at $\delta =$ 0.92–2.80 ppm (*i.e.*, h–m in Fig. 3(III)), and the protons of phenyl rings of polystyrene at $\delta = 6.33$–7.31 ppm (*i.e.*, c and d in Fig. 3(III)), which substantiated the successful coupling of the P(S-N_3) backbone with ethynyl-terminated P3HT side chains. In addition, on the basis of the ^{1}H-NMR analysis of the PS-*g*-P3HT copolymer brush and P(S-Cl), the efficiency of click reaction can be calculated as follows

$$E_T = \frac{M_{n,NMR,PS\text{-}g\text{-}P3HT} - \frac{M_{n,NMR,P(S\text{-}Cl)}}{152.62} \times 159.2}{\frac{M_{n,NMR,P(S\text{-}Cl)}}{152.62} \times M_{n,P3HT}} \times 100\% \quad (1)$$

where E_T is the reaction efficiency of click reaction, 152.62 and 159.2 are the MWs of 4-(chloromethyl)styrene and 4-(azidemethyl)styrene, respectively. $M_{n,NMR,P(S\text{-}Cl)}$, $M_{n,NMR,PS\text{-}g\text{-}P3HT}$ and $M_{n,P3HT}$ are the number-average MWs (M_n) of P(S-Cl) (Table 1), PS-*g*-P3HT (Table 2), and P3HT calculated from ^{1}H-NMR, respectively. All calculated E_T values are nearly 100% (Table 2), clearly suggesting that almost all the coupling sites (–N_3) of P(S-N_3) participated in the click reaction. The success of click reaction was further supported by the IR spectra (Fig. S2†). Obviously, compared with the IR spectrum of P(S-N_3), the characteristic stretching band of –N_3 at 2112 cm^{-1} disappeared, implying that the –N_3 groups took part in the click reaction.

In order to ensure each coupling site (*i.e.*, –N_3) of the P(S-N_3) backbone coupled with one P3HT side chain, ethynyl-terminated P3HT was fed slightly in excess as compared to that of P(S-N_3). The molar ratio of ethynyl-terminated P3HT to –N_3 in P(S-N_3) was about 1.2 : 1. Because the difference in MWs between excessive ethynyl-terminated P3HT and the final product PS-*g*-P3HT was very large, the excess amount of ethynyl-terminated P3HT can be easily removed from the mixture by the fractional precipitation, using THF as a solvent and methanol as a non-solvent, after the click reaction was complete. The GPC curves of the PS-*g*-P3HT copolymer brush and the corresponding constituents (*i.e.*, P(S-Cl) and ethynyl-terminated P3HT) showed singlet and low PDI ($M_w/M_n < 1.2$) (Fig. 4). It is not surprising that the MW of PS-*g*-P3HT from GPC was different from the value derived from ^{1}H-NMR due to the different hydrodynamic volume of the copolymer brush as compared to the linear polystyrene standard (Table 2).

Self-assembly of novel PS-*g*-P3HT copolymer brushes at the air/water interface formed by the Langmuir–Blodgett (LB) technique

The self-assembly of PS-*g*-P3HT copolymer brushes at the air/water interface was then explored using the Langmuir–Blodgett (LB) technique. In contrast to conventional film preparation methods, such as drop-casting and spin-coating, the organization of molecules at the air/water interface can be readily altered by varying the surface pressure, temperature, pH of the water subphase, *etc.*[57] To date, *little* work has been reported on self-assembly of conjugated copolymers at the air/water interface. Nonetheless, the use of LB technique on conjugated polymers has produced a variety of optical and electronic ultrathin film devices, such as thin film conductors.[58] For the copolymer brushes, the presence of joints, branches, and a low level of entanglements offer increased parameters to modify the hydrophobic–hydrophilic balance, thereby enabling the controlled self-assembly process and thus the organized LB film.

The Langmuir isotherm, *i.e.*, surface pressure–area (π–A) plot, of the PS-*g*-P3HT copolymer brushes (sample-b in Table 2) is shown in Fig. S3.† The continuous pressure rise was indicative of the formation of the Langmuir monolayer. Compared

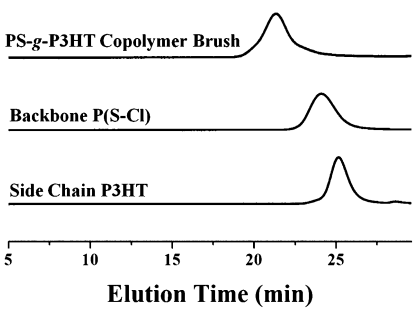

Fig. 4 GPC traces of the P(S-Cl) backbone (*i.e.*, sample-2 in Table 1, M_n = 14 400 g mol^{-1}), P3HT (M_n = 4100 g mol^{-1}) side chains, and the resulting PS-*g*-P3HT copolymer brush (*i.e.*, sample-b in Table 2, M_n = 64 600 g mol^{-1}).

with the reported hydrophobic block copolymers of any structure, which usually exhibit no plateau region in the π–A curves,[59] a long plateau was clearly observed in the isotherm of the PS-*g*-P3HT copolymer brush. Thus, in addition to the gas state (*i.e.*, zero pressure region), the entire isotherm can be divided into three regions: (I) liquid state, (II) plateau region at $\pi = 2$ mN m^{-1} and (III) condensed state. Representative AFM height images and TEM micrographs of thin Langmuir films obtained in these three regions are shown in Fig. 5. Due to their highly localized electron density, P3HT aggregates can be directly imaged by TEM without staining. As a result, all morphological features in TEM images originated solely from the P3HT phase.

The circular and ribbon-like morphologies were seen at the surface pressure of $\pi = 0$ mN m^{-1} (*i.e.*, gas state region, Fig. S4†). Since pressure was not applied, the aggregation of copolymer was a direct consequence of the spontaneous self assembly process. The driving force for the self-assembly was an interplay of the attractive interaction between hydrophilic units (*i.e.*, S atom) on the P3HT chains and the water phase, and the repulsive interaction between PS chains and water as well as between the PS chain and P3HT chains as chloroform evaporated.[60] The corresponding TEM images indicated that the ribbon-like morphology was formed by the chaining of circular domains. Such morphology resembled those structures formed by the dewetting process. When the PS-*g*-P3HT chloroform solution was placed on the water surface, it formed a thin continuous liquid film (1 μm thick, which was calculated by dividing the solution volume (15 μL) by the surface area of the LB trough (160 cm^2)), stabilized by the positive spreading coefficient of chloroform on water.[61] As the solvent evaporated, the liquid film became thinner (<100 nm), and the increased contribution from the unfavorable interfacial interaction between the PS backbone and water eventually resulted in the dewetting of thin film. The dewetting of thin film can be proceeded *via* three stages.[62] First, the film ruptures, thereby generating randomly distributed holes. Second, the holes then grow and the rims ahead of the holes eventually merge to form a cellular structure containing ribbons. Third, the resulting ribbons in the cellular surface morphology are unstable and decay into droplets. It is clear that the observed ribbon-like morphology resembled the morphology formed in the second stage of the dewetting process.[61] As the holes grew during the solvent evaporation, the concentration of PS-*g*-P3HT was greatly increased, leading to the aggregation of polymers and thus the formation of circular and ribbon-like morphologies to reduce the overall free energy of the system.

As the surface pressure increased (*i.e.*, in the liquid state region), the morphology did not change much, with only the increase in domain density due to reduced surface area. Both circular and ribbon-like domains were observed (Fig. 5a and b). In the plateau region, the number of ribbon-like morphology was reduced, and the domain density was increased. As discussed above, the ribbon-like morphology resulted from the chaining of circular domain during the dewetting. Under the surface pressure, the chain can be readily broken, and the large empty space that originally existed between these elongated structures was then filled with the circular domains (Fig. 5c and d). Consequently, a long plateau region resulted most likely due to such rearrangement of circular domains. At the end of the plateau region, the circular domains were highly compact and no longer compressible, thereby leading to a dramatic pressure increase as shown in the condensed state region of the isotherm. During this process, the circular domains appeared much larger than those in the plateau region, signifying that the coalescence of domains occurred (Fig. 5e and f).

A close-up TEM image clearly showed that the domain was composed of fiber-like assemblies (Fig. 6a). It is noteworthy that the nano-sized fiber-like morphology has rarely been reported in the LB study of conjugated polymers; only a wire-like structure has been reported by collapsing a monolayer of amphiphilic polythiophene on the LB trough.[62] The fiber-like morphology has been broadly observed in the *crystalline* state of conjugated rod–coil block copolymers, which self-assembled head-to-tail or head-to-head into various structures, such as nemetic, smectic, hockey pucks, *etc.*[63] By contrast, the spectroscopic measurements on these self-assembled PS-*g*-P3HT copolymer brushes in the condensed state region showed that these nanoscopic fiber-like P3HT did not exist in their *crystalline* state after drying. The photoluminescence (PL) spectra of PS-*g*-P3HT nanofibers and P3HT homopolymer with a MW

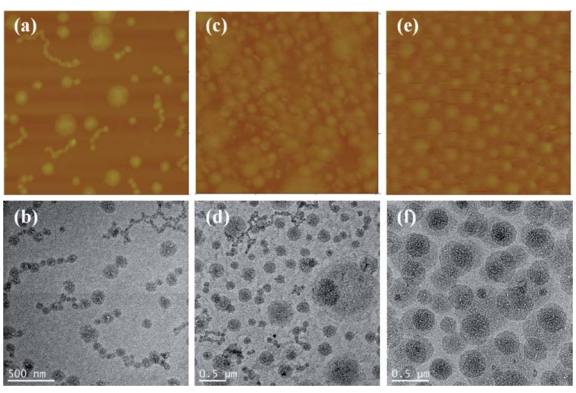

Fig. 5 AFM height images and TEM micrographs of thin Langmuir films obtained from the PS-*g*-P3HT chloroform solution at various transfer pressures (*i.e.*, sample-b in Table 2). (a and b): liquid state region; (c and d): plateau region; and (e and f) condensed state region. Scan size = 3 μm × 3 μm, and *z* scale = 50 nm for all AFM images. Scale bar of TEM images: (b) 500 nm; (d) 0.5 μm; and (f) 0.5 μm.

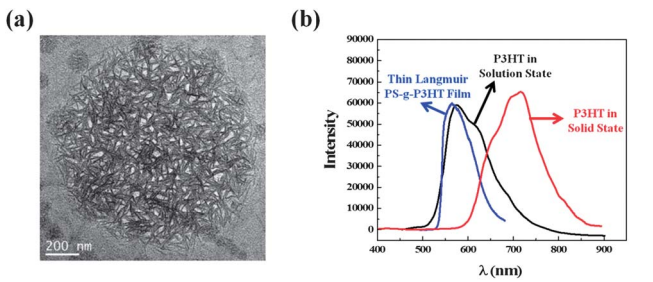

Fig. 6 (a) A close-up TEM image of circular domain obtained in the condensed state region (*i.e.*, from sample-b in Table 2), (b) Photoluminescence spectra of the thin Langmuir film obtained in the condensed state region (blue), and the P3HT homopolymer in the solution state (black) and solid state (red).

identical to individual P3HT chain grafted in PS-*g*-P3HT in both solution and solid states served as references and are shown in Fig. 6b. The vibronic structures of the P3HT homopolymer were clearly evident (*i.e.*, 0–0 emission peak at $\lambda = 574$ nm and 0–1 emission peak at $\lambda = 620$ nm for the solution state; and 0–0 emission peak at $\lambda = 655$ nm and 0–1 emission peak at $\lambda = 715$ nm for the solid state).[64] The electronic structure and optical properties of P3HT have been intensely researched over the past few decades.[65] Two basic types of emission have been identified, namely, intramolecular emission and interchain emission. The 0–0 emission is broadly attributed to the intramolecular interaction, while 0–1 emission is strongly related to the interchain interaction.[66]

In the present study, for the P3HT homopolymer in the solution state, the conjugated chain was broken into conformational subunits, consisting of several repeat units long owing to the relatively low energy barrier for small-angle rotations around bonds along the backbone.[67] Therefore, the emission was blue-shifted due to the reduced conjugated length. Upon drying, the aggregation of P3HT chains, *e.g.*, crystallization, markedly increased the ordering of polymer chains and the degree of interchain interaction, leading to increased conjugated length (*i.e.*, a red-shift) and enhanced 0–1 peak intensity relative to the 0–0 peak, respectively (Fig. 6b). In stark contrast to the crystallized P3HT homopolymer in the solid state, the PS-*g*-P3HT nanofibers in the dry state displayed a similar 0–0 emission position to the coil-like P3HT chains in their solution state (Fig. 6b), suggesting the direct transfer of the disordered state (*i.e.*, non-crystallized) in PS-*g*-P3HT to its solid Langmuir thin film. Moreover, the 0–1 emission peak (approximately at $\lambda = 620$ nm; corresponding to the interchain interaction[66]) relative to 0–0 emission (approximately at $\lambda = 574$ nm) was also dramatically decreased, even negligible (Fig. 6b), which provided clear evidence of prohibited interchain energy transfer.[68] Due to the steric crowding of rod-like P3HT chains on the PS backbone, the hexyl side chains on P3HT may repulse one another, disrupting the effective P3HT interchain π–π stacking. Taken together, the P3HT side chains in the assemblies did not exist in their crystalline state. Nonetheless, this quite intriguing observation will be the subject of further study by capitalizing on grazing-incidence X-ray diffraction.

Conclusions

In summary, novel copolymer brushes, PS-*g*-P3HT, composed of a PS backbone and P3HT side chains were successfully synthesized *via* a rational combination of RAFT polymerization, GRIM, and click reaction. The polymerization of 4-(chloromethyl)styrene was highly controllable. The resulting main chain polymers (*i.e.*, P(S-Cl)) and copolymer brushes possessed a narrow MW distribution; the MW of main chain polymers can be well controlled by changing the reaction time in the RAFT polymerization. The present synthetic approach is simple yet robust and can be extended to create diverse copolymer brushes with different conformations of backbone and side chain (*i.e.*, backbone-*g*-side chain = coil-*g*-coil, coil-*g*-rod, and rod-*g*-rod), hydrophilicity (*i.e.*, hydrophilic, hydrophobic, and amphiphilic) and functions (*i.e.*, luminescent, semiconducting, stimuli-responsive (*e.g.*, thermal, pH, and light), *etc.*) for fundamental study of the relationship between the macromolecular architecture (as well as nanostructured complex assembly yielded upon them) and property in solution and solid states. The self-assembly of PS-*g*-P3HT copolymer brushes at the air/water interface was also explored. Remarkably, circular domain arrays composed of the P3HT nanofibers were observed at high surface pressure. The possible models were proposed to understand the self-assembly and associated photophysical behaviors. We envision that this new class of semiconducting P3HT-containing copolymer brushes may have potential applications in optical sensors and solar cells, among other areas.

Acknowledgements

We gratefully acknowledge funding support from the Air Force Office of Scientific Research (FA9550-09-1-0388) and Georgia Institute of Technology.

Notes and references

1 H. I. Lee, J. Pietrasik, S. S. Sheiko and K. Matyjaszewski, *Prog. Polym. Sci.*, 2010, **35**, 24–44.
2 S. Rathgeber, T. Pakula, A. Wilk, K. Matyjaszewski and K. L. Beers, *J. Chem. Phys.*, 2005, **122**, 1–13.
3 L. H. He, J. Huang, Y. M. Chen, X. J. Xu and L. P. Liu, *Macromolecules*, 2005, **38**, 3845–3851.
4 D. Neugebauer, Y. Zhang, T. Pakula, S. S. Sheiko and K. Matyjaszewski, *Macromolecules*, 2003, **36**, 6746–6755.
5 J. Rzayev, *Macromolecules*, 2009, **42**, 2135–2141.
6 I. Park, S. S. Sheiko, A. Nese and K. Matyjaszewski, *Macromolecules*, 2009, **42**, 1805–1807.
7 M. F. Zhang, C. Estournes, W. Bietsch and A. H. E. Muller, *Adv. Funct. Mater.*, 2004, **14**, 871–882.
8 K. Huang and J. Rzayev, *J. Am. Chem. Soc.*, 2009, **131**, 6880–6885.
9 M. Zhang and A. H. E. Müller, *J. Polym. Sci., Part A: Polym. Chem.*, 2005, **43**, 3461–3481.
10 A. Dag, H. Sahin, H. Durmaz, G. Hizal and U. Tunca, *J. Polym. Sci., Part A: Polym. Chem.*, 2011, **49**, 886–892.
11 M. Xie, J. Dang, H. Han, W. Wang, J. Liu, X. He and Y. Zhang, *Macromolecules*, 2008, **41**, 9004–9010.
12 C. W. Bielawski and R. H. Grubbs, Living Ring-Opening Metathesis Polymerization, in *Controlled and Living Polymerizations*, Wiley-VCH Verlag GmbH & Co. KGaA, 2010, pp. 297–342.
13 S.-H. Lee, M. Ouchi and M. Sawamoto, *Macromolecules*, 2012, **45**, 3702–3710.
14 K. Nakatani, T. Terashima and M. Sawamoto, *J. Am. Chem. Soc.*, 2009, **131**, 13600–13601.
15 M. Ouchi, T. Terashima and M. Sawamoto, *ChemInform*, 2010, **41**, 1–2.
16 K. Matyjaszewski and N. V. Tsarevsky, *Nat. Chem.*, 2009, **1**, 276–288.
17 T. E. Patten and K. Matyjaszewski, *Adv. Mater.*, 1998, **10**, 901–915.

18 Z. Jia, Q. Fu and J. Huang, *J. Polym. Sci., Part A: Polym. Chem.*, 2006, **44**, 3836–3842.
19 C. J. Hawker, G. G. Barclay, A. Orellana, J. Dao and W. Devonport, *Macromolecules*, 1996, **29**, 5245–5254.
20 C. J. Hawker, A. W. Bosman and E. Harth, *Chem. Rev.*, 2001, **101**, 3661–3688.
21 G. Moad, R. T. A. Mayadunne, E. Rizzardo, M. Skidmore and S. H. Thang, *Macromol. Symp.*, 2003, **192**, 1–12.
22 R. T. A. Mayadunne, E. Rizzardo, J. Chiefari, Y. K. Chong, G. Moad and S. H. Thang, *Macromolecules*, 1999, **32**, 6977–6980.
23 S. Perrier and P. Takolpuckdee, *J. Polym. Sci., Part A: Polym. Chem.*, 2005, **43**, 5347–5393.
24 A. B. Lowe, B. S. Sumerlin, M. S. Donovan and C. L. McCormick, *J. Am. Chem. Soc.*, 2002, **124**, 11562–11563.
25 Z. Li, P. Li and J. Huang, *J. Polym. Sci., Part A: Polym. Chem.*, 2006, **44**, 4361–4371.
26 X. Xu and J. Huang, *J. Polym. Sci., Part A: Polym. Chem.*, 2006, **44**, 467–476.
27 G. Moad, R. T. A. Mayadunne, E. Rizzardo, M. Skidmore and S. H. Thang, *Macromol. Symp.*, 2003, **192**, 1–12.
28 B. J. Schwartz, *Annu. Rev. Phys. Chem.*, 2003, **54**, 141.
29 M. C. Iovu, C. R. Craley, M. Jeffries-El, A. B. Krankowski, R. Zhang, T. Kowalewski and R. D. McCullough, *Macromolecules*, 2007, **40**, 4733–4735.
30 M. C. Iovu, M. Jeffries-El, E. E. Sheina, J. R. Cooper and R. D. McCullough, *Polymer*, 2005, **46**, 8582–8586.
31 M. C. Iovu, E. E. Sheina, R. R. Gil and R. D. McCullough, *Macromolecules*, 2005, **38**, 8649–8656.
32 E. E. Sheina, J. S. Liu, M. C. Iovu, D. W. Laird and R. D. McCullough, *Macromolecules*, 2004, **37**, 3526–3528.
33 A. Bhuwalka, J. F. Mike, M. He, J. J. Intemann, T. Nelson, M. D. Ewan, R. A. Roggers, Z. Lin and M. Jeffries-El, *Macromolecules*, 2011, **44**, 9611–9617.
34 C. Y. Liu, Z. C. Holman and U. R. Kortshagen, *Nano Lett.*, 2008, **9**, 449–452.
35 H. Yan and Y. Huang, *Chem. Commun.*, 2011, **47**, 4168–4170.
36 M. C. Stefan, M. P. Bhatt, P. Sista and H. D. Magurudeniya, *Polym. Chem.*, 2012, **3**, 1693–1701.
37 M. Jeffries-El, G. Sauve and R. D. McCullough, *Adv. Mater.*, 2004, **16**, 1017–1022.
38 M. He, J. Ge, Z. Lin, X. Feng, X. Wang, H. Lu, Y. Yang and F. Qiu, *Energy Environ. Sci.*, 2012, **5**, 8351–8358.
39 M. He, W. Han, J. Ge, W. Yu, Y. Yang, F. Qiu and Z. Lin, *Nanoscale*, 2011, **3**, 3159–3163.
40 M. He, L. Zhao, J. Wang, W. Han, Y. Yang, F. Qiu and Z. Lin, *ACS Nano*, 2010, **4**, 3241–3247.
41 M. Byun, R. L. Laskowski, M. He, F. Qiu, M. Jeffries-El and Z. Lin, *Soft Matter*, 2009, **5**, 1583–1586.
42 N. Khanduyeva, V. Senkovskyy, T. Beryozkina, M. Horecha, M. Stamm, C. Uhrich, M. Riede, K. Leo and A. Kiriy, *J. Am. Chem. Soc.*, 2008, **131**, 153–161.
43 N. Khanduyeva, V. Senkovskyy, T. Beryozkina, V. Bocharova, F. Simon, M. Nitschke, M. Stamm, R. Grötzschel and A. Kiriy, *Macromolecules*, 2008, **41**, 7383–7389.
44 H. Sirringhaus, N. Tessler and R. H. Friend, *Science*, 1998, **280**, 1741–1744.
45 Z. Lin, *Chem.–Eur. J.*, 2008, **14**, 6294–6301.
46 V. Senkovskyy, N. Khanduyeva, H. Komber, U. Oertel, M. Stamm, D. Kuckling and A. Kiriy, *J. Am. Chem. Soc.*, 2007, **129**, 6626–6632.
47 P. Paoprasert, J. W. Spalenka, D. L. Peterson, R. E. Ruther, R. J. Hamers, P. G. Evans and P. Gopalan, *J. Mater. Chem.*, 2010, **20**, 2651–2658.
48 H. C. Kolb, M. G. Finn and K. B. Sharpless, *Angew. Chem., Int. Ed.*, 2001, **40**, 2004–2021.
49 P. Wu, A. K. Feldman, A. K. Nugent, C. J. Hawker, A. Scheel, B. Voit, J. Pyun, J. M. J. Fréchet, K. B. Sharpless and V. V. Fokin, *Angew. Chem., Int. Ed.*, 2004, **43**, 3928–3932.
50 W. H. Binder and R. Sachsenhofer, *Macromol. Rapid Commun.*, 2007, **28**, 15–54.
51 S. Oae, T. Yagihara and T. Okabe, *Tetrahedron*, 1972, **28**, 3203–3216.
52 Z. Guo, Y. Feng, Y. Wang, J. Wang, Y. Wu and Y. Zhang, *Chem. Commun.*, 2011, **47**, 9348–9350.
53 M. Yoo, S. Kim, J. Lim, E. J. Kramer, C. J. Hawker, B. J. Kim and J. Bang, *Macromolecules*, 2010, **43**, 3570–3575.
54 M. C. Iovu, E. E. Sheina, R. R. Gil and R. D. McCullough, *Macromolecules*, 2005, **38**, 8649–8656.
55 R. Miyakoshi, A. Yokoyama and T. Yokozawa, *J. Am. Chem. Soc.*, 2005, **127**, 17542–17547.
56 H. Gao and K. Matyjaszewski, *J. Am. Chem. Soc.*, 2007, **129**, 6633–6639.
57 J. Y. Park, N. Koenen, M. Forster, R. Ponnapati, U. Scherf and R. Advincula, *Macromolecules*, 2008, **41**, 6169–6175.
58 M. Rikukawa, M. Nakagawa, H. Abe, K. Ishida, K. Sanui and N. Ogata, *Thin Solid Films*, 1996, **273**, 240–244.
59 L. Zhao, M. Byun, J. Rzayev and Z. Q. Lin, *Macromolecules*, 2009, **42**, 9027–9033.
60 H. B. Wang, W. You, P. Jiang, L. P. Yu and H. H. Wang, *Chem.–Eur. J.*, 2004, **10**, 986–993.
61 P. Muller-Buschbaum, *J. Phys.: Condens. Matter*, 2003, **15**, R1549–R1582.
62 T. Bjornholm, T. Hassenkam, D. R. Greve, R. D. McCullough, M. Jayaraman, S. M. Savoy, C. E. Jones and J. T. McDevitt, *Adv. Mater.*, 1999, **11**, 1218–1221.
63 F. J. M. Hoeben, P. Jonkheijm, E. W. Meijer and A. P. H. J. Schenning, *Chem. Rev.*, 2005, **105**, 1491–1546.
64 J. Xu, J. Wang, M. Mitchell, P. Mukherjee, M. Jeffries-EL, J. W. Petrich and Z. Q. Lin, *J. Am. Chem. Soc.*, 2007, **129**, 12828–12833.
65 I. F. Perepichka, D. F. Perepichka, H. Meng and F. Wudl, *Adv. Mater.*, 2005, **17**, 2281–2305.
66 H. Yamagata and F. C. Spano, *J. Chem. Phys.*, 2012, **136**, 184901.
67 E. Collini and G. D. Scholes, *Science*, 2009, **323**, 369–373.
68 A. Ruseckas, E. B. Namdas, T. Ganguly, M. Theander, M. Svensson, M. R. Andersson, O. Inganas and V. Sundstrom, *J. Phys. Chem. B*, 2001, **105**, 7624–7631.

